

SIMULATION OF PARTICLE PRECIPITATION AND EMISSION PROCESSES IN ELECTRON AURORAS

Kunizo ONDA^{1,2} and Yukikazu ITIKAWA²

¹*Faculty of Industrial Science and Technology, Science University of Tokyo, Oshamanbe, Yamakoshi-gun, Hokkaido 049-35*

²*Institute of Space and Astronautical Science, Yoshinodai, Sagami-hara 229*

Abstract: Electron auroras are theoretically investigated by using the Monte Carlo method. The MSIS-86 model is employed to represent the atmospheric number density and temperature corresponding to the aurora observed at around latitude 58° and longitude 142° on October 21, 1989. Only N_2 , O and O_2 are taken into account as components of the atmosphere. Electrons are injected downward into the upper atmosphere at the altitude of 400 km. The initial electron energy E_0 is considered to be 100 and 500 eV. It is assumed that the initial pitch angle is uniformly distributed. Emission rates for the red and green lines of atomic oxygen, and the first negative band system of nitrogen molecular ions, are specifically calculated as a function of altitude and the initial electron energy. The photo-emission of the red line dominates over that of the green line or those from the first negative band system, if the emission occurs at altitude above 280 km and the initial energy of the precipitating electrons is below a few hundred eV. These results serve as a qualitative model to understand the characteristic features seen in the low latitude electron auroras.

1. Introduction

Electrons precipitating with energy up to a few tens of keV produce a large number of ionizations, excitations, and dissociations of molecules in the upper atmosphere of the earth. These elementary processes result in a variety of electron auroras. Model calculations on electron transport and energy deposition of auroral electrons have been carried out by many workers. We only mention a very limited number of original works, *i.e.*, those of REES (1963), BANKS *et al.* (1974), STRICKLAND *et al.* (1976), SOLOMON *et al.* (1988), and LINK (1992), and some review papers related to electron auroras written by REES (1969, 1987), REES and ROBLE (1975), TORR and TORR (1982), and SOLOMON (1991).

In some auroras, the intensity of the red line emitted from atomic oxygen is almost always much stronger than that of the green line emitted from the same atom or that of the first positive band system of N_2 and the first negative band system of N_2^+ . This type of aurora is often observed at regions in low latitude. It is interesting to know under what conditions of atmospheric structure (chemical composition, number density and temperature as functions of altitude), of the magnetic field, and of the precipitating electrons (energy and pitch-angle distributions and the total flux

as functions of time) this type of aurora appears.

It is the main purpose of this work to calculate the intensity of radiative emissions in the electron aurora as a function of height, and to clarify relations between the relative strength of the red line, the green line, and the emission of the first negative band system of N_2^+ and the energy and pitch angle distributions of the precipitating electrons. Here, we report our preliminary results obtained for some representative values of initial energy and pitch angle of precipitating electrons. These results promise to be helpful in understanding the underlying physics of a low latitude electron aurora. Extended and full results will be presented elsewhere.

Our calculation is based on the Monte Carlo method. This method has been applied to electron transport problems related to electron auroras by BERGER *et al.* (1970), CICERONE and BOWHILL (1971), JACKMAN and GREEN (1979), and very recently SOLOMON (1993) and SERGIENKO and IVANOV (1993). These studies have employed empirically fitted formulas (JACKMAN and GREEN (1979) and YUROVA and IVANOV (1989)) for the electron scattering cross sections from N_2 , O_2 , and O gases. Results of the Monte Carlo calculations are sensitive to the cross sections employed, specifically for excitation processes with low excitation energies such as those of $O(^1D)$ and $O(^1S)$. Therefore, in the low energy region, we have employed digitized data, as detailed as possible for the cross sections. We plan to investigate the dependence of the resulting excitation rate on the cross sections employed. A brief outline of our method is described in the next section (see ONDA *et al.*, 1992) in detail. We have chosen the MSIS-86 model of HEDIN (1983, 1987) for the atmosphere at around latitude 58° and longitude 142° on October 21, 1989. The data sets of the collision cross sections between electrons and N_2 , O , and O_2 , which are the main components of the atmosphere, are adopted from the data compilations by ITIKAWA *et al.* (1986, 1989) and ITIKAWA and ICHIMURA (1990).

2. Calculations

2.1. Electron trajectory and collision processes

The geomagnetic lines of force are regarded as approximately straight in the altitude range from 100 to 400 km. The z axis of our coordinate system is taken along the line of force. The motion of an electron (mass m , charge q) is determined by solving the classical equation of motion:

$$m \frac{d\mathbf{v}}{dt} = q\mathbf{F} + q\mathbf{v} \times \mathbf{B}, \quad (1)$$

where \mathbf{v} is the electron velocity, and \mathbf{F} and \mathbf{B} are the electric (neglected in this work) and magnetic fields, respectively. MKS units are used throughout the present paper. The electron motion during free motion is described by solutions to eq. (1).

The following four procedures are carried out in the Monte Carlo method by using random numbers created on a computer: (A) *Decision of occurrence of collision*; (B) *Decision of type of collision target*; (C) *Decision of type of collision process*; and (D) *Decision of the scattering direction*. The details of these procedures

are described in the ISAS report by ONDA *et al.* (1992).

The electron energy after an inelastic collision is given by $E_f = E_i - \Delta E$, where E_i is the energy before the collision and ΔE is the energy loss in the collision. The energy loss for an ionizing collision is the sum of the relevant ionization energy and the kinetic energy of the secondary electron. The energy loss for an elastic collision is given by the momentum-transfer loss $\Delta E = (2m/M_j)(1 - \cos\omega)E_i$, where M_j is the mass of the j th particle, and ω is the scattering angle.

When the target is a molecule, N_2 or O_2 , we use an approximate analytic expression (OPAL *et al.*, 1971, 1972) of the energy distribution of secondary-electrons in the form:

$$f(\varepsilon) = \frac{C}{1 + (\varepsilon/\zeta)^{2.1}}, \quad (2)$$

where ε is the energy of the ejected electron, ζ is a constant (12.7 eV for N_2 and 17.5 eV for O_2) and C is the normalization constant. For atomic oxygen, we have no experimental data for $f(\varepsilon)$. We use the same $f(\varepsilon)$ as for O_2 .

2.2. Initial conditions for the electron precipitation and termination of the calculation

The initial conditions are expressed as the following parameters: (1) altitude h_0 where the electrons are injected downward into atmosphere; (2) energy E_0 of the electrons; (3) pitch angle α , which is the angle between the initial electron velocity and the geomagnetic line of force; (4) angle β between the local line of force and the vertical.

As soon as the electron energy falls below 2 eV, we stop tracing that electron.

2.3. The atmosphere model and the set of collision cross sections adopted

The MSIS-86 model is adopted to represent atmospheric number densities and temperatures for aurora observed at around latitude 58° and longitude 142° on October 21, 1989. Only N_2 , O and O_2 are taken into account in this work. The number densities of these elements are shown in Fig. 1. The exospheric temperature is $T_{ex} = 1250.18$ K, F107 = 207, and F107A = 219 in this model.

In addition to the momentum transfer in elastic collisions, the excitation of discrete levels and ionization with or without excitation of residual ions are considered for each neutral component of the atmosphere. The number of states taken into account in this work is 16 for N_2 , 11 for O, and 8 for O_2 (see ONDA *et al.*, 1992) in detail. Three electronic states of N_2^+ are distinguished in ionizing collisions of N_2 . For O and O_2 , however, we did not distinguish the ion states. The values of the relevant cross sections used in this work are those reported in the data reviews by ITIKAWA *et al.* (1986, 1989), and by ITIKAWA and ICHIMURA (1990).

The energy loss of the precipitating electrons due to collisions with ambient ionospheric electrons is neglected in this work. This is permissible because the rate of energy loss is orders of magnitude smaller than that of excitation of atoms and molecules in the atmosphere, at least in the energy range above 2 eV.

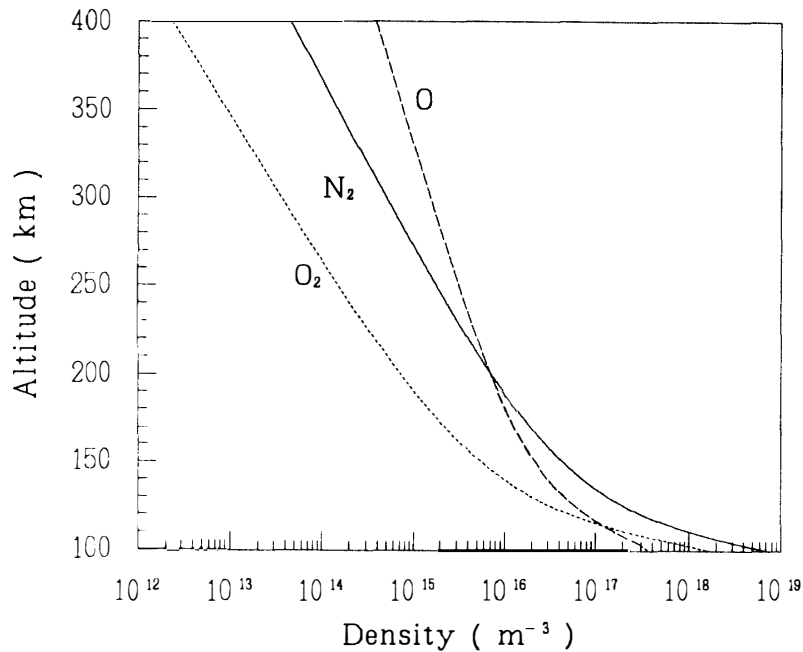


Fig. 1. Altitude distribution of number densities of N_2 , O , and O_2 in the MSIS-86 model atmosphere.

3. Results and Discussion

Calculations have been carried out under the following initial conditions of precipitating electrons: height $h_0 = 400$ km (this value is chosen because the mean free path of electrons having $E_0 = 100$ eV at height $h_0 = 500$ km is estimated to be about 210 km in our model atmosphere), energy $E_0 = 100$ and 500 eV, pitch angle $\alpha = 0^\circ$, and angle between the local line of force and the vertical $\beta = 60^\circ$. These values are chosen from consideration of actual low latitude electron auroras. Since this set of initial conditions is not exhaustive, we do not compare our numerical results with observations. Rather, we try to confirm whether our numerical results are physically reasonable and help us understand the physics of low latitude auroras or not.

3.1. Electron-ion pair production

The number of electron-ion pairs produced per primary electron is shown as a function of altitude for $E_0 = 100$ and 500 eV in Figs. 2 and 3, respectively. Solid lines represent the results of the Monte Carlo calculation. Dashed curves are the results obtained by the continuous-slowing-down (CSD) model calculation (see TAKAYANAGI, 1984; ONDA *et al.*, 1992) for details. The thick short dashed curves represent the contribution from the primary electron; the sum of contributions from both the primary and the secondary electrons is shown by the thin long dashed curves in Fig. 3 and in the following figures.

As shown in Fig. 2a, there is no contribution of the secondary electrons to ionization at $E_0 = 100$ eV. The CSD calculation fails to predict the ionization rate as

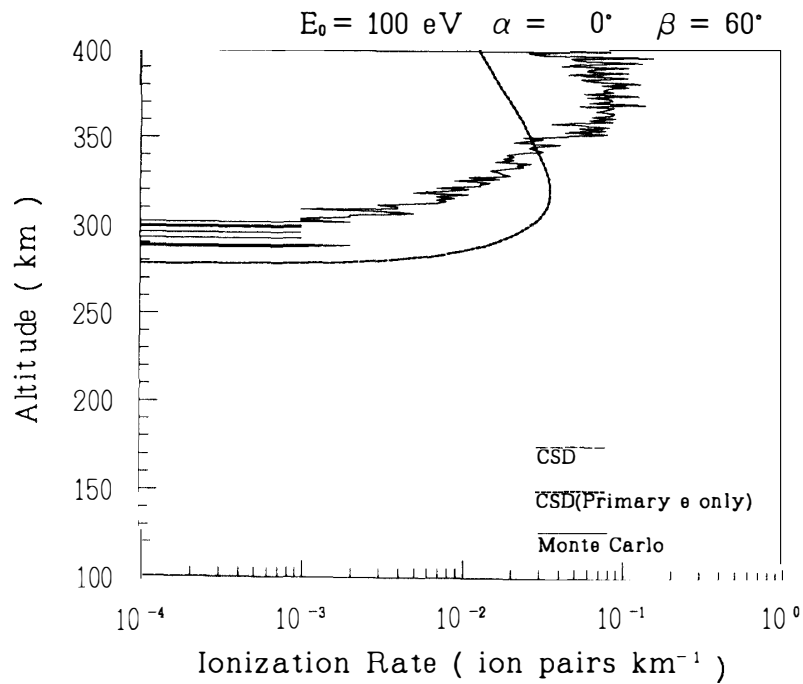


Fig. 2a. Altitude distribution of the ion-electron pairs produced per primary electron. The solid line is the result of the Monte Carlo calculation; long and short dashed lines are for the CSD approximation. $E_0=100 \text{ eV}$, $\alpha=0^\circ$, and $\beta=60^\circ$.

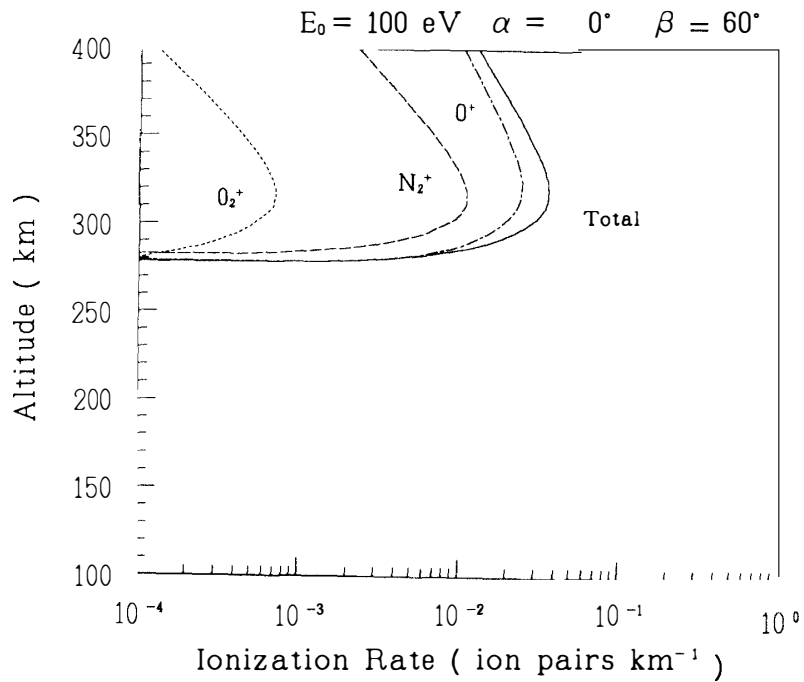


Fig. 2b. Altitude distribution of the ions N_2^+ , O^+ , and O_2^+ produced per primary electron and their sum. The results are obtained by the CSD approximation. $E_0=100 \text{ eV}$, $\alpha=0^\circ$, and $\beta=60^\circ$.

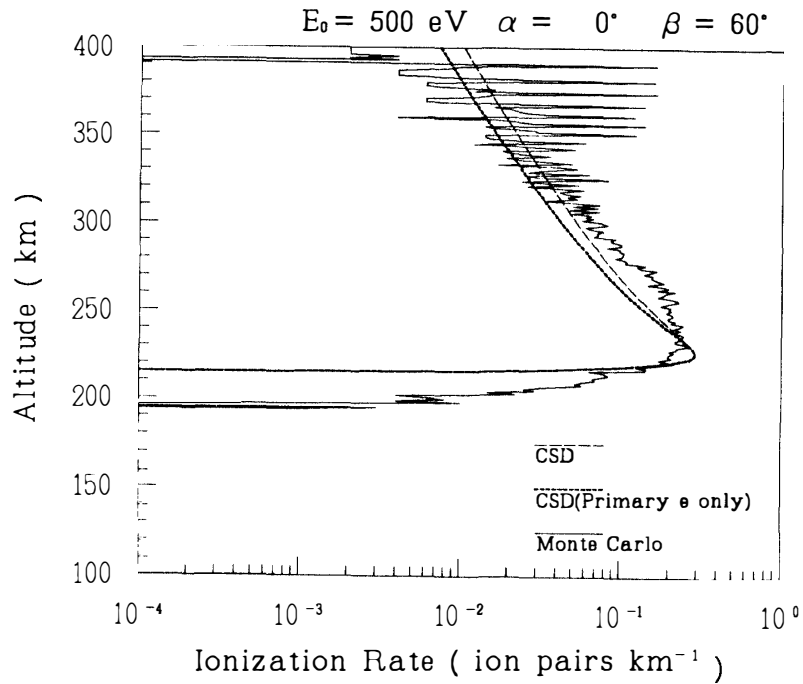


Fig. 3a. Same as Fig. 2a but $E_0 = 500 \text{ eV}$.

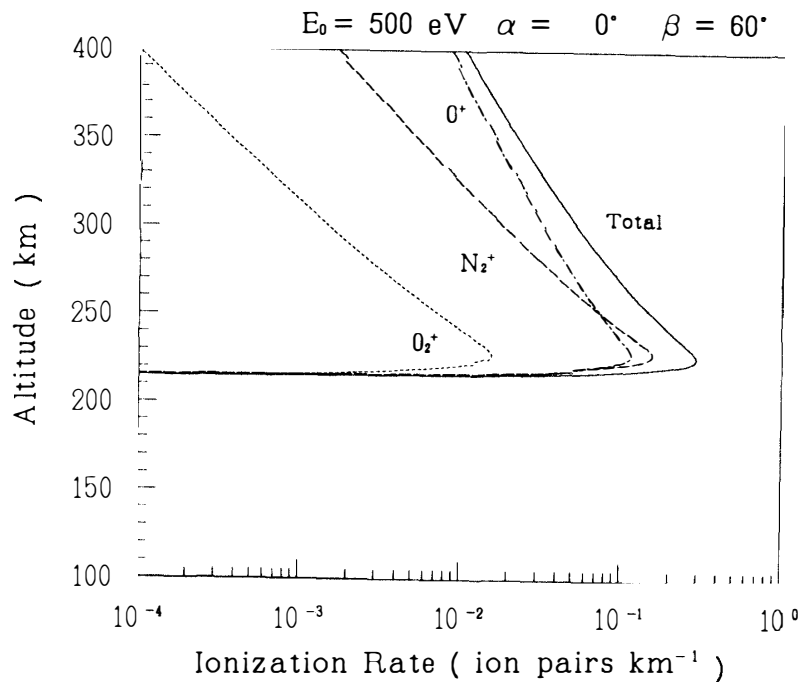


Fig. 3b. Same as Fig. 2b but $E_0 = 500 \text{ eV}$.

a function of height at this energy. On the other hand, if the energy is increased to $E_0 = 500 \text{ eV}$, the CSD model succeeds in reproducing the ionization rate as shown in Fig. 3a, except for the lowest region (below 215 km). At that energy the contribution of the secondary electrons is at most about 20%. As can be understood from Figs. 2b and 3b, contribution from ionization of oxygen atoms dominates over those

from O_2 and N_2 , when the altitude is higher than 250 km and the incident energy is below 500 eV. This is a characteristic feature in this energy range.

3.2. Photo-emission processes

The number of emissions in the first negative band system of N_2^+ [$B^2\Sigma_u^+ \rightarrow X^2\Sigma_g^+$] per primary electron is shown at $E_0=100$ and 500 eV in Figs. 4a and b, respectively. Since the radiative lifetime of the upper states $B^2\Sigma_u^+$ is on the order of several tens of picoseconds, there is no collisional quenching effect to be taken into account. The excitation of the (0,0) band with wavelength around 391.4 nm is nearly 65% of the total excitation of the B states. At $E_0=100$ eV, the excitation of the B state is rare, and the statistical error is large in the Monte Carlo calculation as seen from Fig. 4a. In the case of $E_0=500$ eV, the emission rate calculated by the CSD model (dashed curves) reasonably agrees with that obtained by the Monte Carlo calculation (solid line) at the altitude of 220–300 km. The contribution to this excitation from the secondary electrons is less than 20% of that from the primary electrons at this altitude. The most intensive emission occurs at altitude 230–280 km. The emission rate is in the range 4×10^{-3} to 1.5×10^{-2} photons/km.

The number of emissions of the oxygen green line [$(2p)^4^1S \rightarrow ^1D$ with wavelength 557.7 nm] per primary electron is presented in Figs. 5a and b for $E_0=100$ and 500 eV, respectively. By taking into account the emission region shown in Figs. 5a and b, the radiative lifetime of the upper state 1S (0.79 s), and the number densities of the components of the atmosphere shown in Fig. 1, it is seen that the collisional quenching effect is negligibly small for this emission. The excitation of this state is also rare at $E_0=100$ eV, leading to poor agreement between the results of the Monte Carlo and the CSD calculations. At $E_0=500$ eV, the agreement of the two calculations is good, except for the lowest region (below 230 km). This emission is predominantly caused by the secondary electrons. The most important emission region is almost the same as that for the first negative band system of N_2^+ , although the excitation mechanism is completely different in these two emission processes. The emission rate is in the range 4×10^{-3} to 1×10^{-2} photons/km.

The number of productions of the excited state $(2p)^4^1D_2$ of atomic oxygen and that of emissions of the oxygen red line [$(2p)^4^1D_2 \rightarrow ^3P_{0,1,2}$ with wavelength ~ 630.0 nm] per primary electron are shown in Figs. 6a and b at $E_0=100$ and 500 eV, respectively. In this emission, the secondary electrons also play a major role in producing this excited state. As can be seen from Fig. 6a, if the incident energy is as low as $E_0=100$ eV, the red line is emitted at altitude above 300 km. In the region below 350 km, only about 40% of the excited state 1D_2 is quenched by collisions (see TAKAYANAGI, 1984; ONDA *et al.*, 1992; STREIT *et al.*, 1976), though the radiative lifetime of this state is as long as 147 s. The emission rate is in the range $(2-5) \times 10^{-2}$ photons/km at the altitude of 350–400 km. In Fig. 6, the thick short dashed curves represent the contribution from the primary electron to the number of productions; the thin long dashed curves show the sum of contributions from both the primary and the secondary electrons to the emission rate; and the thin short dashed curves represent the contribution from the primary electrons to the emission

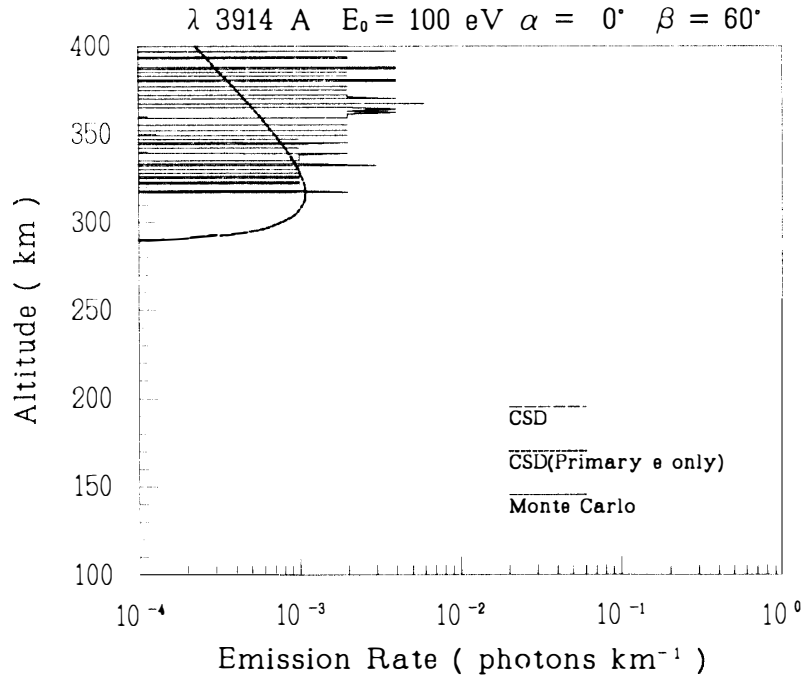


Fig. 4a. Altitude distribution of the photon emissions of the first negative band system of N_2^+ per primary electron. The solid line is the result of the Monte Carlo calculation and the long and short dash lines are those of the CSD approximation. $E_0 = 100$ eV, $\alpha = 0^\circ$, and $\beta = 60^\circ$.

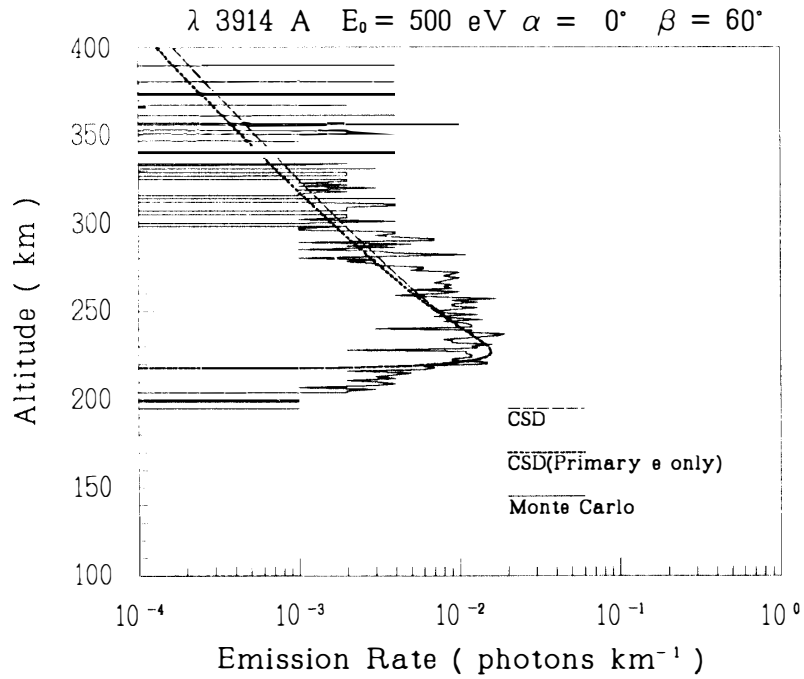


Fig. 4b. Same as Fig. 4a but $E_0 = 500$ eV.

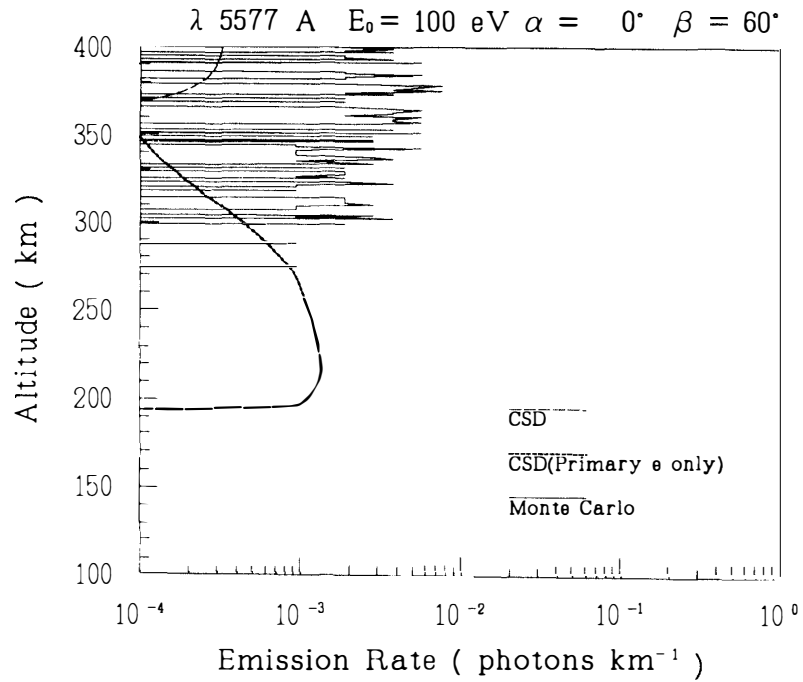


Fig. 5a. Altitude distribution of the photon emissions of the oxygen green line. The solid line is the result of the Monte Carlo calculation and the long and short dashed lines are those of the CSD approximation. $E_0 = 100$ eV, $\alpha = 0^\circ$, and $\beta = 60^\circ$.

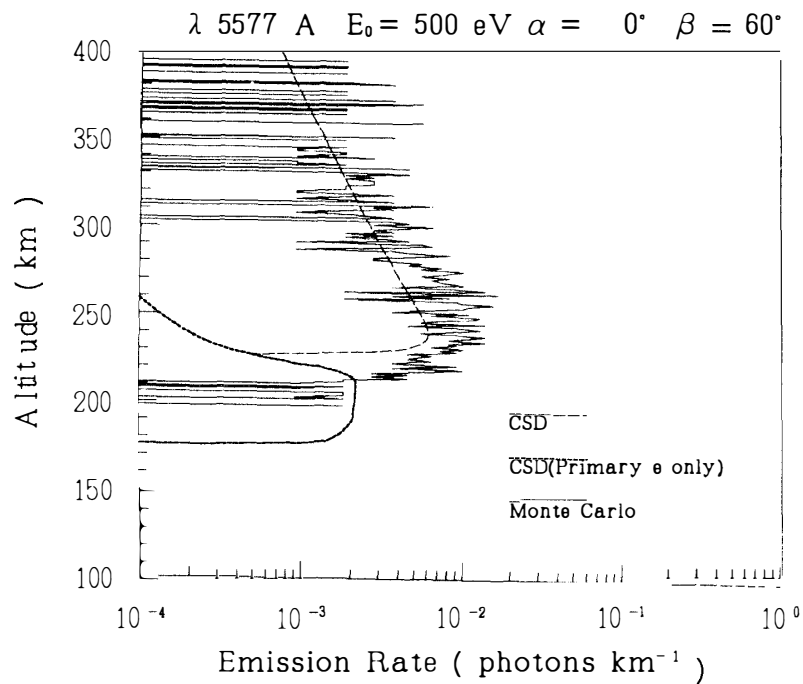


Fig. 5b. Same as Fig. 5a but $E_0 = 500$ eV.

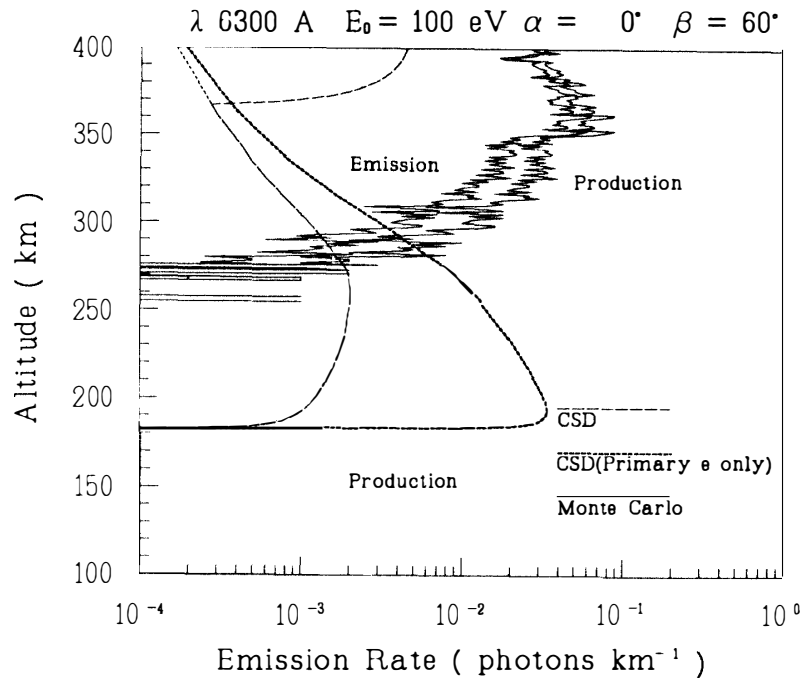


Fig. 6a. Altitude distribution of the $O(^1D)$ production and the emission of the oxygen red line, both per primary electron. The solid lines are the results of the Monte Carlo calculation. The thick short dashed line represents the contribution from primary electrons to production, the thin long dashed line shows the emission rate including both primary and the secondary electron contributions, and the thin short dashed line represents the contribution from the primary electron to the emission rate. The results represented by these dashed lines are calculated by the CSD approximation. $E_0 = 100$ eV, $\alpha = 0^\circ$, and $\beta = 60^\circ$.

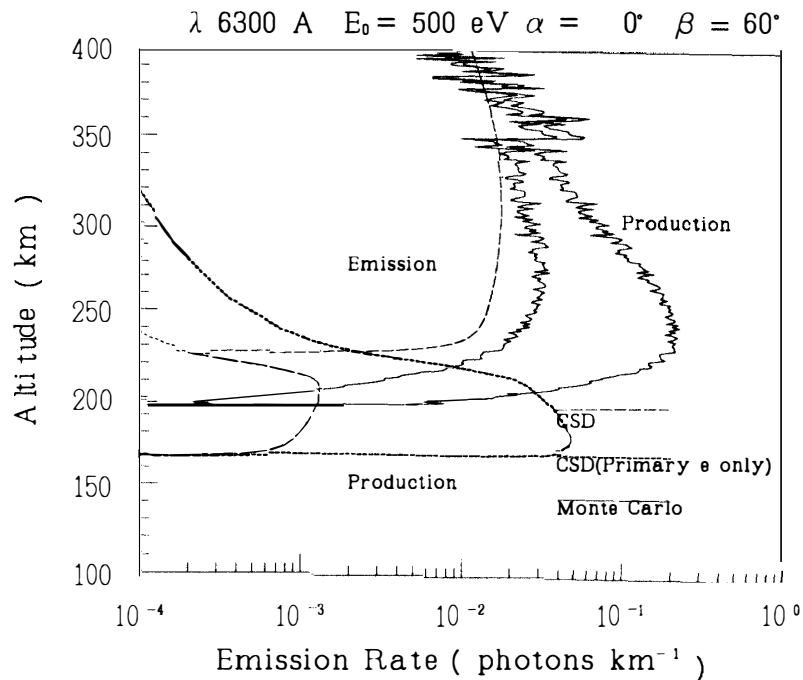


Fig. 6b. Same as Fig. 6a but $E_0 = 500$ eV.

rate. These results are calculated by using the CSD method. This figure clearly shows that the energy loss of the primary electrons is not correctly taken into account in the CSD calculations at altitude above 300 km. Thus, the primary electrons can come down to the altitude at about 185 km. This is the main reason why the CSD calculations fail to estimate the height distribution of both the production and the following emission rates at this incident energy of $E_0 = 100$ eV. As the energy is increased to $E_0 = 500$ eV, the emission region is extended over 230–400 km, and, depending on the altitude, about (85–40)% of the excited atoms are collisionally quenched. The emission rate is in the range $(2-3.5) \times 10^{-2}$ photons/km. At altitude above 230 km, it is favorable for the excited state 1D_2 to emit the red line, because the effect of collisional quenching is minor there. The CSD calculations reasonably reproduce the emission rate as shown by the thin long dashed curve in Fig. 6b except in the lowest part of this altitude region. As can be seen from this figure, the energy loss of the primary electrons is still not properly taken into account in the CSD calculations, even at incident energy $E_0 = 500$ eV.

From the present investigation, it is quite reasonable to draw the conclusion that the red line can be stronger by a factor of (5–10) than the green one and the one with wavelength 391.4 nm, if the emission region is above 280 km and the initial energy of precipitating electrons is below 500 eV.

Here, we have specifically investigated the case of the pitch angle $\alpha = 0^\circ$. As the pitch angle is increased from 0° to 90° , precipitating electrons will lose their energy more quickly at the higher altitude compared with the case of $\alpha = 0^\circ$. Therefore, the excited state $O(^1D_2)$ will emit the red line without appreciable collisional quenching compared with the case of $\alpha = 0^\circ$, and the above conclusion becomes more probable after summing up over the pitch angle distribution.

4. Concluding Remarks

We have reported the results of simulation of particle precipitation and emission processes in electron auroras by using the Monte Carlo method. Our results show that the oxygen red line emission can be the strongest in electron auroras in the altitude range 280–400 km. These events can be produced by electrons precipitating with initial energy below a few hundred eV.

In our calculations, other production mechanisms of the excited state $O(^1D_2)$, such as dissociation of oxygen molecules by electron impact and dissociative recombination of oxygen molecular ions, are not taken into account. Qualitative justification of our results is understood from the following consideration. The ratio of number density of oxygen molecules to that of oxygen atoms is smaller than 10^{-2} at altitude higher than 250 km as can be estimated from Fig. 1. Therefore, the contribution from the processes mentioned above to the emission of the 630.0 nm line is considered to be negligible. A similar argument is applicable to other production mechanisms of excited $O(^1S)$ and $N_2^+(B^2\Sigma_u^+)$. Above 250 km, other ion-molecule and chemical reaction processes become rare, and can be neglected. A quantitative study of the effects of these processes on electron auroras is in planning.

Acknowledgments

This work is performed as one of the cooperative projects at NIPR. The authors express their sincere thanks to Prof. M. EJIRI and Dr. H. MIYAOKA of NIPR for suggesting this subject and encouragement during this study. Numerical calculations have been carried out using the FACOM M-780/20, VP-200, and VPP-500 at the Computer Center, ISAS.

References

- BANKS, P. M., CHAPPELL, C. R. and NAGY, A. F. (1974): A new model for the interaction of auroral electrons with the atmosphere: Spectral degradation, backscatter, optical emission, and ionization. *J. Geophys. Res.*, **79**, 1459–1470.
- BERGER, M. J., SELTZER, S. M. and MAEDA, K. (1970): Energy deposition by auroral electrons in the atmosphere. *J. Atmos. Terr. Phys.*, **32**, 1015–1045.
- CICERONE, R. J. and BOWHILL, S. A. (1971): Photoelectron fluxes in the ionosphere computed by a Monte Carlo method. *J. Geophys. Res.*, **76**, 8299–8317.
- HEDIN, A. E. (1983): A revised thermospheric model based on mass spectrometer and incoherent scatter data: MSIA-83. *J. Geophys. Res.*, **88**, 10170–10188.
- HEDIN, A. E. (1987): MSIS-86 thermospheric model. *J. Geophys. Res.*, **92**, 4649–4662.
- ITIKAWA, Y. and ICHIMURA, A. (1990): Cross sections for collisions of electrons and photons with atomic oxygen. *J. Phys. Chem. Ref. Data*, **19**, 637–651.
- ITIKAWA, Y., HAYASHI, M., ICHIMURA, A., ONDA, K., SAKIMOTO, K. *et al.* (1986): Cross sections for collisions of electrons and photons with nitrogen molecules. *J. Phys. Chem. Ref. Data*, **15**, 985–1010.
- ITIKAWA, Y., ICHIMURA, A., ONDA, K., SAKIMOTO, K., TAKAYANAGI, K. *et al.* (1989): Cross sections for collisions of electrons and photons with oxygen molecules. *J. Phys. Chem. Ref. Data*, **18**, 23–42.
- JACKMAN, C. H. and GREEN, A. E. S. (1979): Electron impact on atmospheric gases. 3. Spatial yield spectra for N₂. *J. Geophys. Res.*, **84**, 2715–2724.
- LINK, R. (1992): Feautrier solution of the electron transport equation. *J. Geophys. Res.*, **97**, 159–169.
- ONDA, K., HAYASHI, M. and TAKAYANAGI, K. (1992): Monte Carlo calculation of ionization and excitation rates in electron aurora. *ISAS Rep.*, **645**, 1–38.
- OPAL, C. B., PETERSON, W. K. and BEATY, E. C. (1971): Measurements of secondary-electron spectra produced by electron impact ionization of a number of simple gases. *J. Chem. Phys.*, **55**, 4100–4106.
- OPAL, C. B., BEATY, E. C. and PETERSON, W. K. (1972): Tables of secondary-electron production cross sections. *Atomic Data*, **4**, 209–253.
- REES, M. H. (1963): Auroral ionization and excitation by incident energetic electrons. *Planet. Space Sci.*, **11**, 1209–1218.
- REES, M. H. (1969): Auroral electrons. *Space Sci. Rev.*, **10**, 413–441.
- REES, M. H. (1987): Modelling of the heating and ionizing of the polar thermosphere by magnetospheric electron and ion precipitation. *Phys. Scri.*, **T18**, 249–255.
- REES, M. H. and ROBLE, R. G. (1975): Observations and theory of the formation of stable auroral red arcs. *Rev. Geophys. Space Phys.*, **13**, 201–242.
- SERGIENKO, T. I. and IVANOV, V. E. (1993): A new approach to calculate the excitation of atmospheric gases by auroral electron impact. *Ann. Geophys.*, **11**, 717–727.
- SOLOMON, S. C. (1991): Optical aeronomy. *Rev. Geophys. Suppl.*, **29**, 1089–1109.
- SOLOMON, S. C. (1993): Auroral electron transport using the Monte Carlo method. *Geophys. Res.*

- Lett., **20**, 185–188.
- SOLOMON, S. C., HAYS, P. B. and ABREU, V. J. (1988): The auroral 6300 Å emission: Observation and modeling. *J. Geophys. Res.*, **93**, 9867–9882.
- STREIT, G. E., HOWARD, C. J., SCHMELTEKOFF, A. L., DAVIDSON, J. A. and SCHIFF, H. I. (1976): Temperature dependence of O(¹D) rate constants for reactions with O₂, N₂, CO₂, O₃, and H₂O. *J. Chem. Phys.*, **65**, 4761–4764.
- STRICKLAND, D. J., BOOK, D. L., COFFEY, T. P. and FEDDER, J. A. (1976): Transport equation techniques for the deposition of auroral electrons. *J. Geophys. Res.*, **81**, 2755–2764.
- TAKAYANAGI, K. (1984): A numerical study of artificial electron aurora experiment. *ISAS Rep.*, **611**, 1–32.
- TORR, M. R. and TORR, D. G. (1982): The role of metastable species in the thermosphere. *Rev. Geophys. Space Phys.*, **20**, 91–144.
- YUROVA, I. Y. and IVANOV, V. E. (1989): *Electron Cross Sections of Atmospheric Gases*. Leningrad, Nauka.

(Received June 3, 1994; Revised manuscript received September 3, 1994)